INTERNATIONAL JOURNAL OF AUTOMOTIVE AND MECHANICAL ENGINEERING
ISSN: 2229-8649 e-ISSN: 2180-1606
VOL. 21, ISSUE 3, 2024, 11712 – 11722
DOI: https://doi.org/10.15282/ijame.21.3.2024.20.0903

RESEARCH ARTICLE

An Investigation of Classical Model Predictive Controller Path Tracking Performance of a Two-Wheel and Four-Wheel Steering Vehicle

H. Che Shamsudin[1], M. I. Ishak[1]*, P. M. Heerwan[1], M. A. Zakaria[2]

[1]Faculty of Mechanical and Automotive Engineering Technology, Universiti Malaysia Pahang Al-Sultan Abdullah, 26600 Pekan, Pahang, Malaysia
[2]Faculty of Manufacturing and Mechatronic Engineering Technology, Universiti Malaysia Pahang Al-Sultan Abdullah, 26600 Pekan, Pahang, Malaysia

ABSTRACT – Studies on self-driving vehicles have become a trend in recent years, and many systems have been developed to enable autonomous manoeuvre. Various methods have been used to improve path-tracking algorithms which increase vehicle performance, including tracking accuracy and stability. Path tracking is one of the primary problems for autonomous vehicles where the vehicle deviates from target paths, which leads to unnecessary counter-correction. Conventional front wheel steering is unable to satisfy the manoeuvre with a high lateral acceleration since the front steering angle is limited in accurately responding to vehicle dynamics. Moreover, the characteristics of front wheel steering vehicles affect handling stability due to the fact that the turning radius is larger than the vehicle itself. This disadvantageous can compromise safety during under-steer and over-steer situations. The main objective of this preliminary study is to investigate the performance of a four-wheel steering system (4WS) in path tracking for autonomous vehicles using a classical model predictive controller (MPC). Conventional two-wheel steering (2WS) tracking performance following the desired driving system with the same MPC controller is compared with 4WS vehicles. The driving system is developed using Driving Scenario Designer to extract the desired yaw angle and lateral position for controller references constructed in Matlab Simulink. Fixed MPC constraint, prediction, control horizon, yaw angle and lateral position weights were used to compare the performance between 2WS and 4WS vehicles. The simulation results show that 4WS is three times better than 2WS vehicles in tracking predetermined paths. 4WS vehicle show 74.55% better performance in lateral position tracking and 68.75% better performance in trailing predetermined yaw angle value. The simulation data from the preliminary study will be used as a guideline to develop an advanced controller of 4WS vehicles.

ARTICLE HISTORY
Received : 25th June 2023
Revised : 17th May 2024
Accepted : 21st Aug. 2024
Published : 07th Oct. 2024

KEYWORDS
Autonomous vehicles
Path tracking control
2WS vs 4WS
Classical MPC

1. INTRODUCTION

Self-driving vehicles, also known as autonomous vehicles or driverless cars, can operate without direct human input. These vehicles use a combination of advanced sensors, cameras, and radar systems [1]–[3]. Artificial intelligence algorithms are applied to perceive the environment by analysing the collected sensor data and making real-time decisions in order to control the vehicle's movements [4], [5]. Nevertheless, the ability to follow a path smoothly and accurately in order to stay on the intended trajectory should be emphasised in the study of autonomous vehicles. The main purpose of the automatic path tracking control system is to ensure autonomous vehicles with dynamic constraints move in a stable condition while following a predetermined path and ensure that lateral position errors are always minimal [6], [7].

In the path tracking controller, the error between the vehicle's actual trajectory and the desired path is minimised by continuously adjusting the vehicle's steering control inputs. Various control algorithms have been developed to improve autonomous vehicles' path tracking and lateral position error performance, namely Pure Pursuit & Stanley, PID controller, LQR controller, Feedforward & feedback control and MPC Controller. Ackerman's steering geometry is exploited to design the Pure Pursuit & Stanley control method. Songxiao Cao et al. proposed path tracking based on the pure pursuit method to calculate the deviation between the current and the reference paths for obtaining the target steering wheel angle and vehicle speed [8]. Ahmad Abdelmoniem et al. analysed the behaviour of autonomous vehicles following different manoeuvre paths based on the Stanley method [9]. The execution of these controllers is straightforward and works well for controlling the vehicle's position. The standard equations do not involve acceleration or force. The controller operates effectively on simple roads and in low-speed circumstances. However, dynamic variables like vehicle acceleration, yaw rate, and tyre force have a significant impact on the path tracking control when the vehicle is operating in a substantial road curve and at high speed. One of the most popular methods in control systems, including path tracking, is PID, which continuously calculates an error value to adjust the system's output to bring the process variable closer to the desired value. Benjamas Panomruttanarug et al. demonstrate level 1 autonomy of autonomous golf carts and lateral tracking control can be achieved using a PID controller [10]. To improve PID controller performance to track the desired path, Xueping Dong et al. [11] proposed a fractional-order PID where a stochastic technique is used to tune the controller parameters. Nonetheless, the PID controller is not adaptable to system alteration. The control parameters are no longer ideal when the operating conditions change dramatically.

***CORRESPONDING AUTHOR | M. I. Ishak** | ✉ mizhar@umpsa.edu.my

On the other hand, the Linear Quadratic Regulator (LQR) is also used for path tracking control, where the system's linear state-space model is utilised to compute the optimal control input in order to minimise a cost function that represents the performance of the system. The findings presented by Y. Sun et al. indicate that the LQR combined with feedback linearisation exhibits enhanced path-tracking performance by optimising control inputs to maintain system stability [12]. Yet, due to linear feedback and model simplification, the effect of the controller is greatly reduced when the vehicle behaves nonlinearly, which involves modelling failures or encountering external disturbances. Due to this, T. Hossain et al., in a study, developed feedforward control based on road information and an LQR controller to generate specific steering angles in order to improve path-tracking performance [13]. While Z. Wang et al. presented an applied real-time fuzzy control method to tune the LQR weight coefficients in addition to feedback-feedforward components, shows better tracking accuracy and steering stability [14]. The problem with this method is the requirement of high computing power since online optimisation is necessary and relies on an accurate mathematical model of the system, which increases measurement cost quantity.

Well, Model predictive control can manage system restrictions and enable future forecasting throughout the design process. The control algorithm has grown to be a common technique for autonomous vehicle control by reducing the difference between the reference path and the actual path of the vehicle in a prediction horizon. The comparison study of unmanned vehicles between LQR and MPC control methods exhibits that MPC controller has better controllability and tracking robustness at different speeds [15]. Linhe Ge et al. use NMPC for motion control of autonomous vehicles to solve the increasing stiffness problem of vehicles at low speeds. The RKC integration method adopted affected the performance of NMPC, and the vehicle successfully completed a U-turn manoeuvre with a small radius at a speed of 0.2 m/s [16]. G. Chen et al. studied the path-tracking method based on the combination of a hierarchical dynamic drifting controller (HDDC) and MPC [17]. The results show that the handling limits of autonomous cars can be significantly increased by high sideslip drifting manoeuvres with the proposed controller.

The path-tracking method mentioned earlier was explicitly developed for traditional two-front-wheel steering (2WS) vehicle systems. 2WS systems may have less stability when travelling at high speeds [18]. The lack of rear-wheel steering input might increase the risk of oversteer [19] or understeer, which can impact the vehicle's overall stability [20]. 2WS also suffers traction and handling restrictions under specific driving circumstances, such as on slippery or uneven terrain, since there is no additional control input from the back wheels [21]. In addition, 2WS vehicles could experience difficulties travelling through severely constrained areas like parking lots or narrow roads. Sharp turns [22] may be more difficult to execute when there is no rear-wheel steering, and some manoeuvres may require recurred manoeuvres to complete. On the contrary, four-wheel steering (4WS) is different from 2WS as there are steering inputs in both the front wheels and rear wheels. The wheels can either be mechanically linked or controlled by steer-by-wire in order to maintain the Instant Centre of Rotation (ICR). Besides eliminating the physical connection between the steering and wheels of the vehicle, using the steer-by-wire system has a higher advantage in fully utilising the 4WS potential. 4WS has a significant advantage of manoeuvrability when compared to 2WS Ackerman due to the decreased radius of the ICR induced by the second steering angle [23].

In the pursuit of impeccable lateral dynamic stability and precise path-tracking performance for 4WS vehicles, numerous controllers have been proposed by dedicated researchers. Trajectory tracking strategy based on the hierarchical control method consists of a path-tracking layer, dynamics control layer and tyre force distribution layer with neural network Proportion Integration Differentiation (NNPID) controller improves the stability and energy saving of the vehicle and effectively reduces tyre wear [24]. In the study by X. Wu et al., the designed autonomous vehicle has excellent ability path tracking, which meets the design goals using fuzzy and a multi-step predictive optimal controller [25]. Model predictive control (MPC) is an essential optimal control technique widely employed for path-tracking control of both linear and nonlinear systems.[26]. The 4WS autonomous vehicle, utilising the MPC controller, vastly improves path-tracking performance compared to other controllers. Additionally, it effectively reduces the likelihood of drifting or veering off the runway at high speeds and on low-adhesion roads.[27], [28]. In addition, MPC controllers are proven to have better performance in trajectory tracking if utilised on 4WS compared to 2WS vehicles, nevertheless under disturbance effect [29].

The present work is the preliminary effort to compare the tracking performance of 4WS with 2WS vehicles using parameters acquired from Proton Persona, UMP test car. It examines the tracking problems where the front and rear steering are adjusted to follow the target path. The rest of this paper is organised as follows: vehicle modelling will be described in the next section, including the kinematics of the bicycle model and the equation of motion used for 2WS and 4WS vehicles. Then, the driving scenario and environment used in this study for testing autonomous driving systems will be explained. MPC controller for path tracking will be shown in the following chapter. Lastly, simulation results obtained and discussions will be shown before the conclusion is made to conclude the overall study.

2. VEHICLE MODELLING

2.1 Kinematics of Bicycle Model

The vehicle model will be represented by a Bicycle model. In normal driving conditions, a classic bicycle model can be used to express vehicle motion. To analyse the kinematics of the bicycle model, the reference point x-y on the vehicle must be selected as either the centre of the rear (CoR) axle, the centre of the front (CoF) axle or the centre of gravity

(CoG). According to Figure 1, the technical parameter of the Malaysian national car, namely the Proton Persona, is chosen for simulation purposes. The reference x-y on the vehicle of the centre of the rear (CoR) axle is selected since the encoder used to collect vehicle velocities is attached to the rear wheel. The lateral velocity, V_x and longitudinal velocity, V_y of the vehicle coordinate frame are calculated using the kinematic equation in (1) and (2):

$$V_x = V \cos\ \theta \tag{1}$$

$$V_y = V \sin\ \theta \tag{2}$$

where *V* is the vehicle's velocity while δ, θ, R, and L are the steering angle, yaw angle, rotation radius and length between wheels of the vehicle.

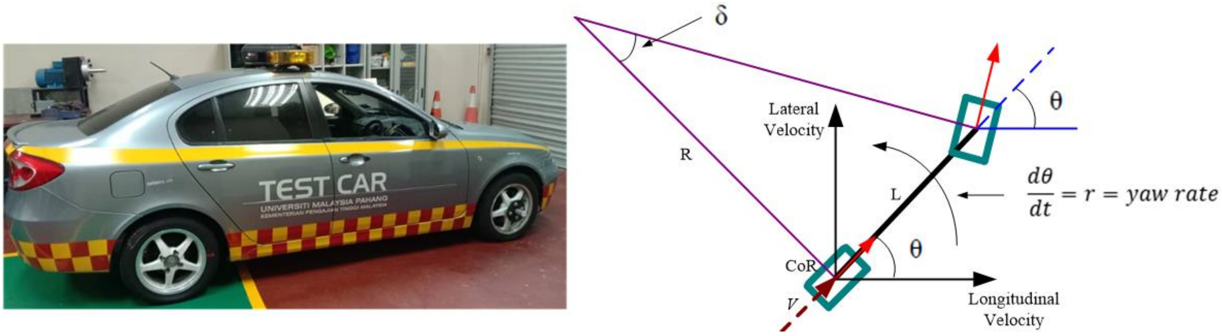

Figure 1. Proton Persona test car with centre of rear axle reference point

2.2 Lateral Equation of Motion

In this study, linear models of 2WS and 4WS are used due to the assumption that there is no coupling between translation and angular velocity by considering the normal condition of the vehicle, as shown in Figure 2.

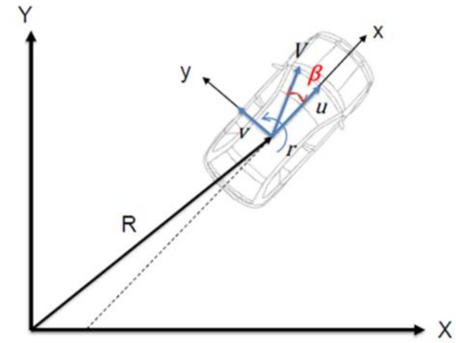

Figure 2. Coordinate frame of vehicle motion

$$if\ u \gg v,\ \ then\ |\beta|\ is\ small \tag{3}$$

$$V = \sqrt{(u^2 + v^2)}\ is\ constant \tag{4}$$

where *u* and *v* are vehicle velocity components on the x and y axes. From equations (3) and (4), the side slip angle is assumed to be small when the vehicle is moving at constant speed since the velocity on the axis is much larger than the velocity on the axis.

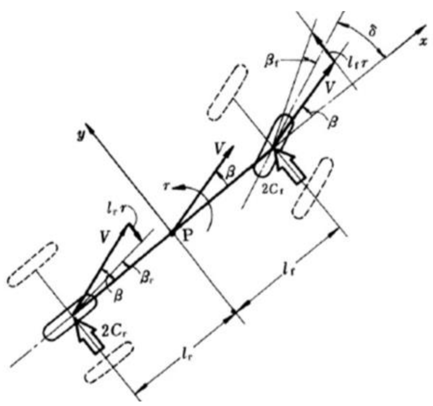

Figure 3. Equivalent bicycle model [30]

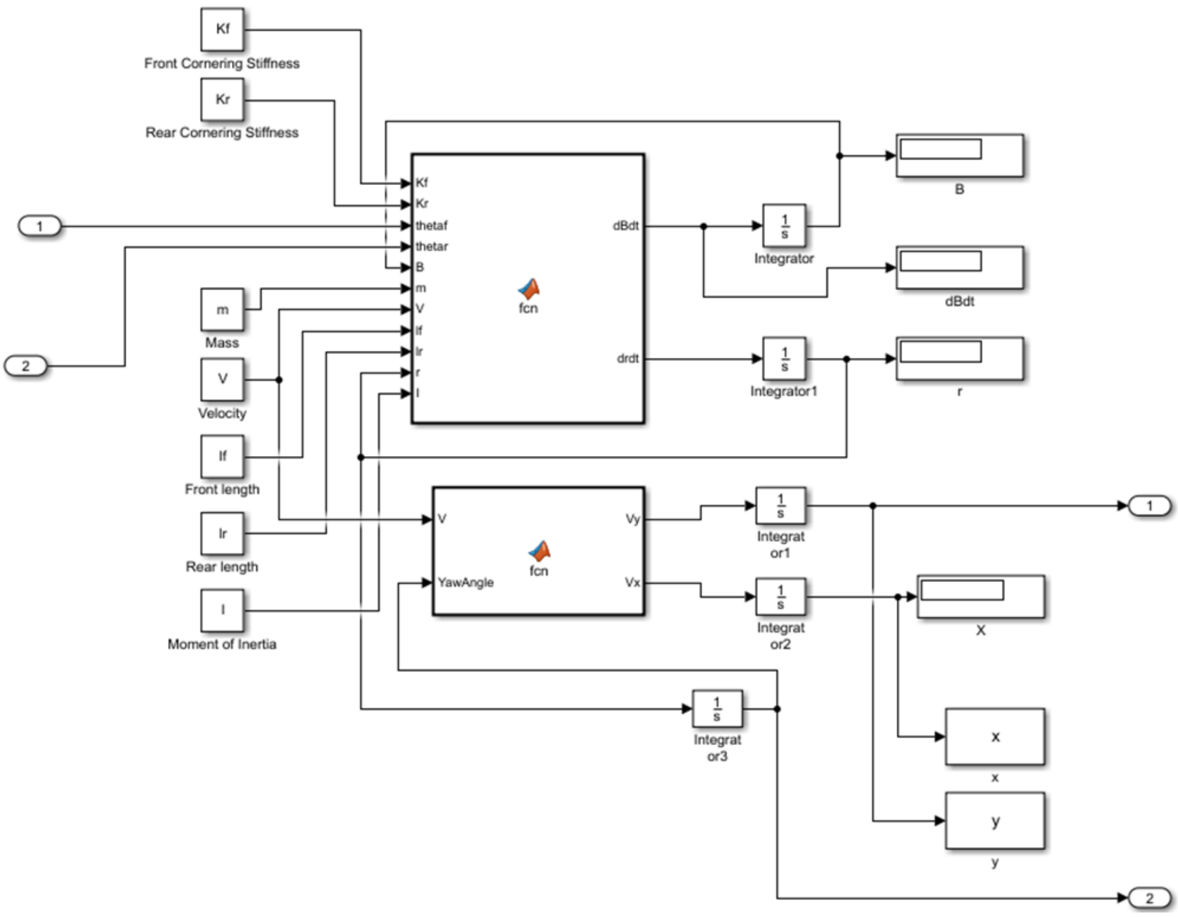

Figure 4. Single Simulink plant system

According to the equivalent bicycle model in Figure 3, the lateral acting forces on the front and rear tyres are Y_f and Y_r. The lateral motion of the vehicle can be calculated by equation (5) and (6).

$$mV\left(\frac{d\beta}{dt}+r\right)=2Y_f+2Y_r \tag{5}$$

$$I\frac{dr}{dt}=2l_fY_f-2l_rY_r \tag{6}$$

where m, I, r, l_f, l_r and δ are the vehicle's mass, yaw moment of inertia, yaw rate, length from the centre of gravity to the front tyre, length from the centre of gravity to the rear tyre and steering angle, respectively. By substituting front and rear cornering stiffness K_f and K_r into lateral acting forces, which are proportional to side slip angle acting on both tyres Bf and Br as shown in equations (7) and (8), the lateral motion of the vehicle equations can be rewritten to (9) and (10).

$$Y_f=-K_fB_f=-K_f\left(\beta+\frac{l_fr}{V}-\delta\right) \tag{7}$$

$$Y_r=-K_rB_r=-K_r\left(\beta-\frac{l_rr}{V}\right) \tag{8}$$

$$mV\left(\frac{d\beta}{dt}+r\right)=-2K_f\left(\beta+\frac{l_fr}{V}-\delta\right)-2K_r\left(\beta-\frac{l_rr}{V}\right) \tag{9}$$

$$I\frac{dr}{dt}=-2K_f\left(\beta+\frac{l_fr}{V}-\delta\right)l_f+2K_r\left(\beta-\frac{l_rr}{V}\right)l_r \tag{10}$$

Equations (7) to (10) are only valid for 2WS vehicles since there is only one steering angle involved. In order to customise with a 4WS vehicle, the front steering angle, δ_f and rear steering angle, δ_r must be included. The vehicle equations of motion in response to front and rear wheel steer are now as shown in equations (11) to (14).

$$Y_f=-K_fB_f=-K_f\left(\beta+\frac{l_fr}{V}-d_f\right) \tag{11}$$

$$Y_r = -K_r B_r = -K_r\left(\beta - \frac{l_r r}{V} - \delta_r\right) \tag{12}$$

$$mV\frac{d\beta}{dt} + 2\left(K_f + K_r\right)B + \left\{mV + \frac{2}{V}\left(l_f K_f - l_r K_r\right)\right\}r = 2K_f\delta_f + 2K_r\delta_r \tag{13}$$

$$2\left(l_f K_f - l_r K_r\right)\beta + I\frac{dr}{dt} + \frac{2\left(l_f^2 K_f + l_r^2 K_r\right)}{V}r = 2l_f K_f\delta_f - 2l_r K_r\delta_r \tag{14}$$

In order to calculate the value of the yaw angle and lateral position value of the 2WS and 4WS models, the kinematic equation of the bicycle model (1) - (2) and vehicle equations of motion (11) - (14) are combined in a single Simulink plant system as shown in Figure 4.

3. DRIVING SCENARIO AND ENVIRONMENT

In order to test the tracking algorithm using a classical MPC controller, data must be tested for analysis. Driving Scenario Design in Matlab is a platform that allows researchers to drive simulation cars over different environments. These applications enable users to create the desired road and add actors to imitate the vehicle movement. In urban environments, the suggested design speed for a single-entry lane is 40–50 km/h, whereas the recommended design speed for the circulatory lane is 20-30 km/h, per article [31]. Since 20 km/h is roughly 5.55556 m/s, there are researchers using 6 m/s for the vehicle's velocity in order to simulate urban driving [32], hardware-in-the-loop simulation [33], validation for automatic steering controller [34] and study of autonomous driving on the slippery road [35]. This study uses a straight road with a roundabout to obtain the trajectory point. According to Figure 5, a single car with a velocity of 6m/s is used as an actor. Simulation at low speed enables the reduction of the slip angle. On the other hand, the test car travelled between 10 to 15 km/h while obtaining values for Proton Persona parameters. Therefore, 6m/s is selected as a nearby velocity value to test the low-speed controller performance for the preliminary study.

The actor is moved through the road following the designated point for approximately 25 seconds to reach the endpoint. After the simulation is complete, all the data regarding actor movement, including travel on the straight lane, lane changing conditions, and following a roundabout, is exported to Matlab. The lateral position and yaw angle data of the actor are extracted to be used as reference values for the MPC controller to control 2WS and 4WS vehicles following the predetermined trajectories.

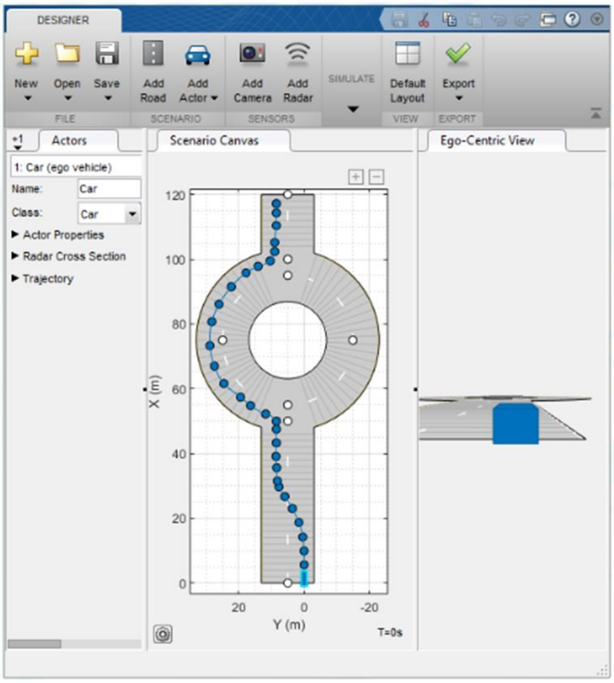

Waypoints

	x (m)	y (m)
1	0	0
2	5.6000	0
3	9.9000	0
4	14.2000	0.4000
5	18.7000	1.6000
6	23	3.6000
7	26.7000	5.9000
8	29.7000	7.7000
9	31.5000	8.2000
10	35.6000	8.4000
11	39.1000	8.6000
12	43.3000	8.5000
13	47.5000	8.5000
14	50	8.5000
15	52.2000	11.8000
16	54.8000	16.4000
17	57.4000	19.5000
18	61.6000	24.6000
19	67	27.5000
20	73.3000	28.9000
21	80.7000	28.3000
22	86.1000	26.1000
23	91.5000	22.3000
24	95.8000	17.8000
25	97.8000	14.1000
26	99.5000	10.4000
27	102.4000	9
28	105.2000	9
29	110.4000	8.5000
30	114.3000	8.5000
31	117.2000	8.5000

Figure 5. Driving scenario design

4. MPC CONTROLLER FOR PATH TRACKING

MPC consists of three main components that control or regulate a plant's system output, which are predictive, feedback correction and optimisation. A prediction horizon can be set to allow the controller to predict the extent to which an event will occur in the future. This controller calculates the error between the output signal and the reference value and uses the cost function to optimise the plant's input signal. It is a naturally multi-input-multi-output (MIMO) controller that enables the combination of multivariable and simple design frameworks to control complex systems successfully.

MPC is widely used to control linear or nonlinear systems with constraints, including path-tracking problems, while preserving system stability.

In this paper, classical model predictive control to regulate the path tracking problem of 2WS and 4WS vehicles is achieved using the Simulink toolbox. Figure 6 illustrates the control structure for 2WS, which uses only front steering, while 4WS utilises both front and rear steering. For the 2WS system with classical MPC, there are two measure outputs (MO), which are lateral position and yaw angle, while the front steering angle is the only manipulated variable (MV). Since the system plant uses the same equations (13)-(14), the second input (rear steering angle) is set to zero. On the other hand, the 4WS system with classical MPC has two MOs similar to 2WS vehicles, but a rear steering angle is available for the second MV. Both MPC controllers are set so that there are no measured disturbances (MD).

After the MPC structure is set up, defined, and linearised, the plant model is executed to enable the controller to run the default simulation scenario. The Input and output response against the internal plant is displayed depending on the selected reference signal, tuning value and desired input-output constraints. Table 1 shows all the parameter values to set the classical MPC controller for the 2WS and 4WS path-tracking problems used in this study.

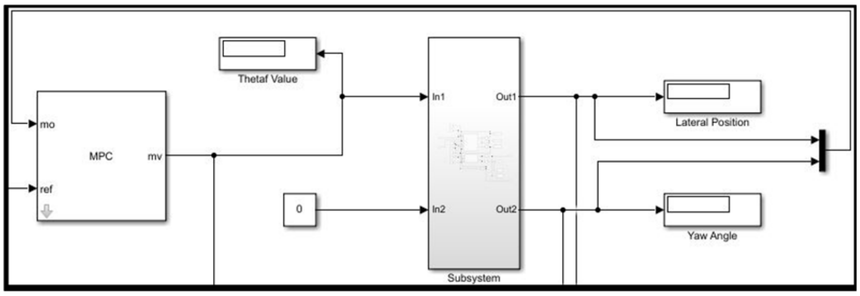

2WS System with Classical MPC

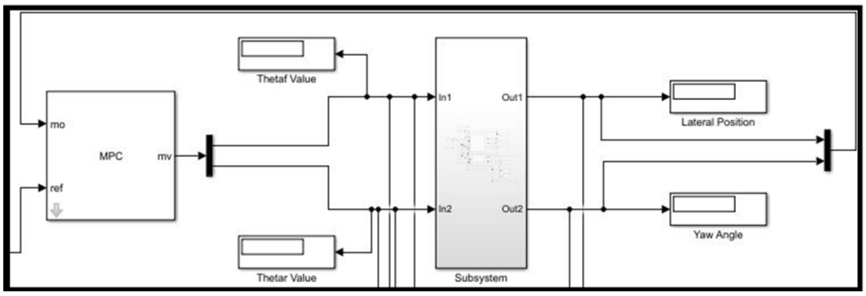

4WS System with Classical MPC

Figure 6. Path tracking control structure for classical MPC

Table 1. Classical MPC Parameter Value for Path Tracking

Setup Parameter	2WS	4WS
Sample Time	0.01s	0.01s
Manipulate Variable (MV)	1	2
Measure Output (MO)	2	2
Prediction Horizon	10	10
Control Horizon	2	2
Input Constraints for MV1	-pi/6 (min), pi/6 (max)	-pi/6 (min), pi/6 (max)
Input Constraints for MV2	-	-pi/6 (min), pi/6 (max)
Output Constraints for MO1	-5 m (min), 30 m (max)	-5 m (min), 30 m (max)
Output Constraints for MO2	-pi/2.6 (min), pi/2.6 (max)	-pi/2.6 (min), pi/2.6 (max)

5. SIMULATION RESULTS

This section discusses the simulation and results. Matlab and Simulink are used to evaluate the performance of 2WS and 4WS vehicle tracking based on predetermined pathways. The yaw moment of inertia and cornering stiffness of the front and rear tyres of the Proton Persona Test Car were obtained from previous research using estimation and identification techniques. The technical specifications of the vehicle used for the simulation purpose are shown in Table 2 [36], [37]. The simulation is done for both vehicles to track predetermined paths at low speeds.

Table 2. Technical specifications of Proton Persona

Parameter	Value
Total vehicle mass, m (kg)	1330
Yaw moment of inertia, i (mns^2)	1335
Longitudinal distance from the centre of gravity to the front tyres, l_f (m)	1.107
Longitudinal distance from the centre of gravity to the rear tyres, l_r (m)	1.643
Cornering stiffness of the front tyres, k_f (N/rad)	75000
Cornering stiffness of the rear tyres, k_r (N/rad)	10650

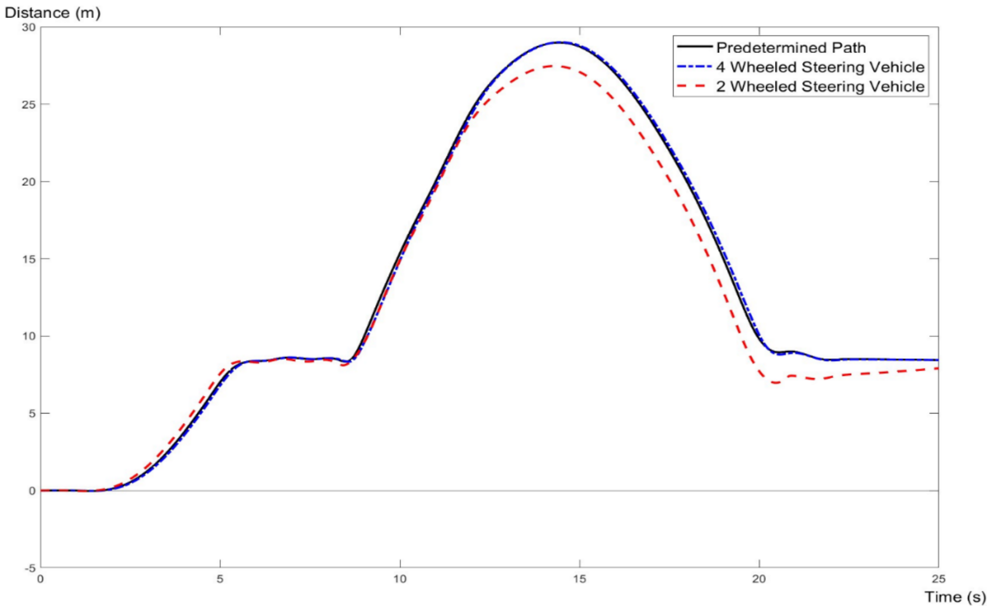

Figure 7. Lateral position tracking performance for both vehicles

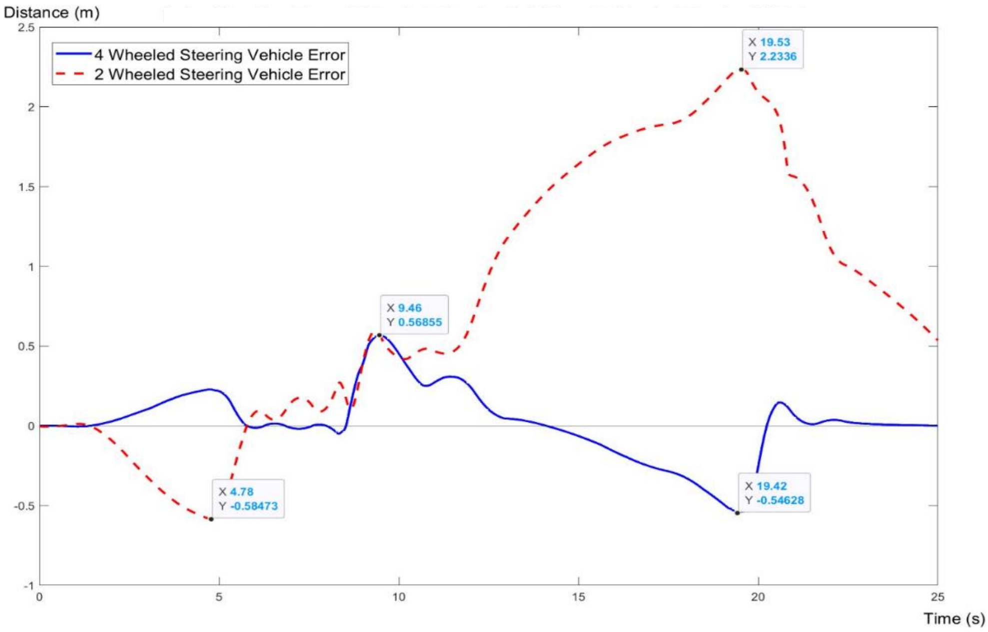

Figure 8. Lateral position error tracking performance for both vehicles

Figure 7 shows the trajectory results for comparison simulation for 2WS and 4WS vehicles within 25 s. The black line represents the desired predetermined path, while the blue line and red dash line are the tracking performance for 2WS and 4WS vehicles, respectively. The Y axis of the graph represents the lateral position of the vehicles in meters, and the X axis shows the simulation time. Lateral position tracking for 4WS vehicles shows better performance in comparison to 2WS vehicles. Tracking performance by both vehicles is similar at the initial t = 10s, which is during the straight lane.

As soon as the 2WS vehicle changes lanes to the left, deviation from the predefined path can be observed while the 4WS vehicle maintains following the predetermined path. On the roundabout, the error for the 2WS vehicle can be observed to increase as the vehicle passes through a curved path to the right. 2WS approached the predetermined path again when the lane was straight at the end of the simulation, while the 4WS vehicle maintained following with low error. According to Figure 8, the maximum error for a 4WS vehicle is 0.5686m compared to 2.2336 m for the 2WS vehicle. From the simulation, it is shown that the 4WS vehicle shows 74.55% better performance for lateral position tracking.

As the 4WS vehicle exhibits better performance in lateral position error while following a predetermined path, the 2WS vehicle continuously shows poor performance from the perspective of the yaw angle result shown in Figure 9. The Y axis of the graph represents the yaw angle value for both vehicles in rads while tracking the predetermined path. The Yaw angle for both vehicles still follows the predetermined yaw angle value for the first eight seconds of the navigation. Then, 2WS vehicle yaw angle performance begins to demonstrate deterioration when the path enters the roundabout curve section. The error continues to remain for the 2WS vehicle until the end of the simulation, while the 4WS vehicle demonstrates high capabilities to follow predetermined yaw angle value. The maximum error for the 4WS vehicle is 10º compared to 32º for the 2WS vehicle. Figure 10 shows that the 4WS vehicle shows 68.75% better performance in trailing predetermined yaw angle value. All the calculated minimum, maximum and root mean square error values to compare the performance between 4WS and 2WS vehicles are shown in Table 3 and Table 4.

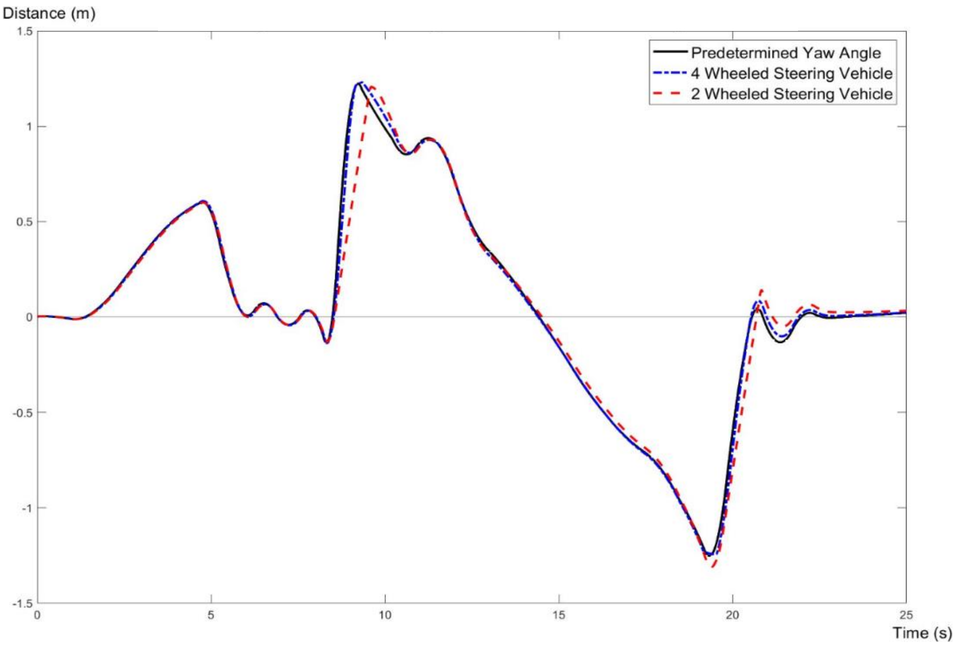

Figure 9. Yaw angle tracking performance for both vehicles

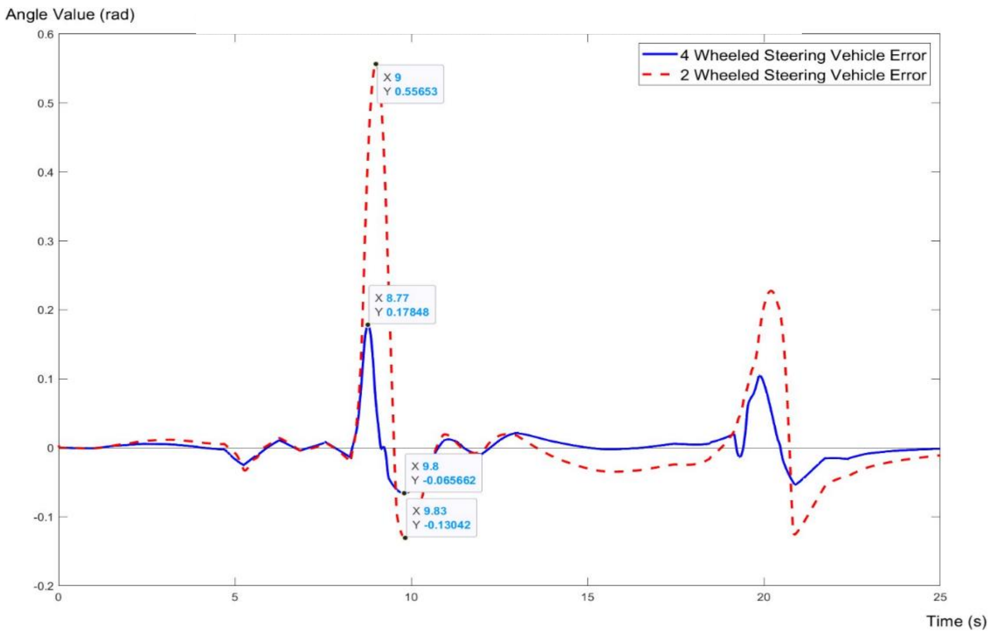

Figure 10. Yaw angle error tracking performance for both vehicles

In order to justify the results of the trajectory and the yaw angle for the 4WS and 2WS vehicles in the path tracking performance, the steering angle input of the vehicle following the predefined pathway should be evaluated, as shown in Figure 11. According to Figure 11, the steering angles of the 4WS vehicle are represented by blue and cyan lines for the front and rear steering angle input, respectively. The red dash line represents only the front steering angle for 2WS vehicles. All the steer turning angles are limited to 0.5236 rad since the maximum tyre's turning angle for the standard car is 30^{o}.

In the case of the 2WS vehicle, the steering angle input has reached maximum value and saturated at t = 8s – 10s and t = 19s – 22s. This supports the error in the trajectory and yaw angle where the vehicle was understeer and unable to follow the predefined pathway. In the case of the 4WS vehicle, the majority of the steering angle of the rear is the opposite value to the front wheel. There are several instances where the steering angles are the same phase (positive or negative) for the front and rear, such as at t = 7s, 9s, and 19s. The MPC controller governs the opposite and parallel steering modes of the 4WS system and continuously changes the modes in order to keep the path tracking error to the minimum value throughout the low-speed manoeuvrability simulation.

Table 3. Trajectory error values for 2WS vehicle

Error Metric	Lateral Position (Y)	Yaw Angle (θ)
Maximum Error	2.2336 m	0.5585 rad
Minimum Error	0	0
Root Mean Square Error	1.1478 m	0.0937 rad

Table 4. Trajectory error values for 4WS vehicle

Error Metric	Lateral Position (Y)	Yaw Angle (θ)
Maximum Error	0.5686 m	0.1745 rad
Minimum Error	0 m	0
Root Mean Square Error	0.2159	0.0291 rad

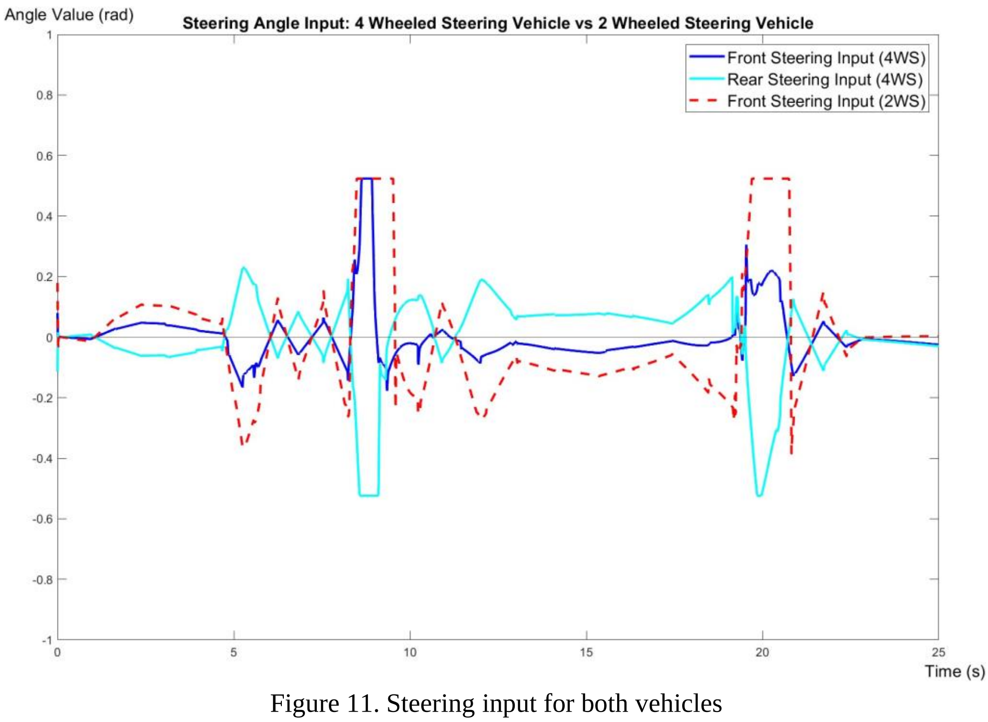

Figure 11. Steering input for both vehicles

Traditionally, the 4WS system was passive, meaning that the rear steering angle was proportional to the front wheel steering angle based on the vehicle's velocity. While effective in certain situations, this approach limited the system's flexibility and responsiveness. However, based on this research, the 4WS system, with the advent of Model Predictive Control (MPC), has become more sophisticated and independent of velocity. MPC allows the system to dynamically adjust the steering modes, switching between parallel and opposite steering based on the lateral position and yaw angle of the path planning input. This advancement enables the vehicle to navigate more complex scenarios with enhanced stability, manoeuvrability, and responsiveness, ultimately improving the overall path-tracking performance.

6. CONCLUSION

This paper reports the first attempt to compare 4WS vehicle that enables them to provide better performance than 2WS vehicle during path tracking, which is one of the most important criteria in autonomous vehicles. Both vehicles' velocity use 6 m/s constant speed in order to demonstrate the continuously-transition mode capability of 4WS vehicle even if the speed does not change. The absence of this feature on 2WS vehicles may cause tracking accuracy to be decreased with speed increase. Although using the classical MPC as a controller, the 4WS vehicle demonstrates 74.55% better performance in lateral position tracking and is three times more accurate than 2WS when tracking the yaw angle value of a predetermined path. The maximum lateral error of the 4WS vehicle in this study is 0.5686m, which is 0.329m smaller compared to the control algorithm for the 2WS vehicle. With an upper limit of 20 km/h for the 2WS vehicle's velocity, the proposed controller recorded a maximum error of 0.8927m, which is also higher than that of the 4WS vehicle. The capability of changing steering angles independently along with dual mode steering, which are opposite and parallel steering for 4WS, has a crucial impact on overall path tracking performance. For future works, it can be extended to apply an adaptive MPC to control autonomous 4WS vehicle in path-tracking problems.

ACKNOWLEDGEMENT

This research was supported by the Ministry of Higher Education Malaysia through the Fundamental Research Grant Scheme FRGS/1/2019/TK08/UMP/02/5. Special thanks to the Automotive Engineering Center (AEC) and Smart Campus Autonomous Vehicle (SCAV) Laboratory, Universiti Malaysia Pahang, for providing facilities and technical support.

REFERENCES

[1] M.H. Le, C.H. Cheng, and D.G. Liu, "An efficient adaptive noise removal filter on range images for LiDAR point clouds," *Electronics*, vol. 12, no. 9, p. 2150, 2023.

[2] W. Kim, H. Yang, and J. Kim, "Blind spot detection radar system design for safe driving of smart vehicles," *Applied Sciences*, vol. 13, no. 10, p. 6147, 2023.

[3] C.H. Shih, C.J. Lin, and J.Y. Jhang, "Ackerman unmanned mobile vehicle based on heterogeneous sensor in navigation control application," *Sensors (Basel)*, vol. 23, no. 9, p. 4558, 2023.

[4] J. Hernandez-Barragan, J.D. Rios, A.Y. Alanis, C. Lopez-Franco, J. Gomez-Avila, and N. Arana-Daniel, "Adaptive single neuron anti-windup PID controller based on the extended Kalman filter algorithm," *Electronics*, vol. 9, no. 4, pp. 18–21, 2020.

[5] L. Wang, J. Zhao, and R. Mortier, "Neural Network," In *OCaml Scientific Computing, Undergraduate Topics in Computer Science*, Springer, Cham. pp. 219-242, 2022.

[6] J. Liu, H. Liu, J. Wang, and H. Gu, "Coordinated lateral stability control of autonomous vehicles based on state estimation and path tracking," *Machines*, vol. 11, no. 3, p. 328, 2023.

[7] H. Shi, G. Geng, X. Xu, J. Xie, and S. He, "Path tracking control of intelligent vehicles considering multi-nonlinear characteristics for dual-motor autonomous steering system," In *Actuators*, vol. 12, no. 3, p. 97, 2023.

[8] S. Cao, Y. Jin, T. Trautmann, and K. Liu, "Design and experiments of autonomous path tracking based on dead reckoning," *Applied Sciences*, vol. 13, no. 1, p. 317, 2023.

[9] A. Abdelmoniem, A. Ali, Y. Taher, M. Abdelaziz, and S.A. Maged, "Fuzzy predictive Stanley lateral controller with adaptive prediction horizon," *Measurement and Control (United Kingdom)*, vol. 56, no. 9-10, pp. 1510-1522, 2023.

[10] B. Panomruttanarug, T. Ketnoi, A.K. Ojha, and N. Boonruam, "Design and development of navigation system for an autonomous vehicle," In *2023 Third International Symposium on Instrumentation, Control, Artificial Intelligence, and Robotics (ICA-SYMP)*, pp. 100–104, 2023.

[11] X. Dong, H. Pei, and M. Gan, "Autonomous vehicle lateral control based on fractional-order PID," *2021 IEEE 5th information technology, networking, electronic and automation control conference*, vol. 5, pp. 830–835, 2021.

[12] Y. Sun, Q. Dai, J. Liu, X. Zhao, and H. Guo, "Intelligent vehicle path tracking based on feedback linearisation and LOR under extreme conditions," *2022 41st Chinese Control Conference*, vol. 2022, pp. 5383–5389, 2022.

[13] T. Hossain, H. Habibullah, and R. Islam, "Steering and speed control system design for autonomous vehicles by developing an optimal hybrid controller to track reference trajectory," *Machines*, vol. 10, no. 6, p. 420, 2022.

[14] Z. Wang, K. Sun, S. Ma, L. Sun, W. Gao, and Z. Dong, "Improved linear quadratic regulator lateral path tracking approach based on a real-time updated algorithm with fuzzy control and cosine similarity for autonomous vehicles," *Electronics*, vol. 11, no. 22, p. 3703, 2022.

[15] Y. Wang, J. Wang, J. Yang, R. Du, Z. Hai, and H. Deng, "Research on path tracking control of unmanned vehicle," *Journal of Physics: Conference Series*, vol. 2480, no. 1, p. 012002, 2023.

[16] L. Ge, Y. Zhao, S. Zhong, Z. Shan, F. Ma, Z. Han et al., "Efficient and integration stable nonlinear model predictive controller for autonomous vehicles based on the stabilised explicit integration method," *Nonlinear Dynamics*, vol. 111, no. 5, pp. 4325–4342, 2023.

[17] G. Chen, X. Zhao, Z. Gao, and M. Hua, "Dynamic drifting control for general path tracking of autonomous vehicles," *IEEE Transactions on Intelligent Vehicles*, vol. 8, no. 3, pp. 2527-2537, 2023.

[18] J. Zhang, H. Zheng, and M. Zhao, *Analysis of vehicle steering stability of nonlinear four wheel steering based on sliding mode control*, SAE Technical Paper, no. 2018-01-1593, 2018.

[19] L. Maoqi, M.I. Ishak, and P.M. Heerwan, "The effect of parallel steering of a four-wheel drive and four-wheel steer electric vehicle during spinning condition: A numerical simulation," *IOP Conference Series: Materials Science and Engineering*, vol. 469, no. 1, p. 012084, 2019.

[20] S. Yim, "Comparison among active front, front independent, 4-wheel and 4-wheel independent steering systems for vehicle stability control," *Electronics*, vol. 9, no. 5, p. 798, 2020.

[21] P. Hang, X. Xia, G. Chen, and X. Chen, "Active safety control of automated electric vehicles at driving limits: A tube-based MPC approach," *IEEE Transactions on Transportation Electrification*, vol. 8, no. 1, pp. 1338–1349, 2022.

[22] M. Shekh, O.P. Umrao, and D. Singh, "Kinematic analysis of steering mechanism: A review," In *Proceedings of International Conference in Mechanical and Energy Technology: ICMET 2019, India*, vol. 174, pp. 529–540, 2020.

[23] D.S. Choudhari, "Four wheel steering system for future," *International Journal of Mechanical Engineering and Robotics Research*, vol. 3, no. 4, pp. 383–387, 2014.

[24] H. Zheng and S. Yang, "A trajectory tracking control strategy of 4WIS/4WID electric vehicle with adaptation of driving conditions," *Applied Sciences*, vol. 9, no. 1, p. 168, 2019.

[25] X. Wu and Y. Yang, "Path tracking controller design of automatic guided vehicle based on four-wheeled omnidirectional motion model," *International Journal of Automotive and Mechanical Engineering*, vol. 17, no. 2, pp. 7996–8010, 2020.

[26] Y. Li *et al.*, "Trajectory tracking of four-wheel driving and steering autonomous vehicle under extreme obstacle avoidance condition," *Vehicle System Dynamics*, vol. 62, no. 3, pp. 601-622, 2023.

[27] R. Liu, M. Wei, N. Sang, and J. Wei, "Research on curved path tracking control for four-wheel steering vehicle considering road adhesion coefficient," *Mathematical Problems in Engineering*, vol. 2020, no. 1, p. 3108589, 2020.

[28] P. Hang, X. Chen, and F. Luo, *Path-tracking controller design for a 4WIS and 4WID electric vehicle with steer-by-wire system*, SAE Technical Paper, no. 2017-01-1954, 2017.

[29] F. Yakub, A. Abu, S. Sarip, and Y. Mori, "Study of model predictive control for path-following autonomous ground vehicle control under crosswind effect," *Journal of Control Science and Engineering*, vol. 2016, no. 1, p. 6752671, 2016.

[30] A. Masato, *Vehicle Handling Dynamics Theory and Application*, First. Oxford: Butterworth-Heinemann, 2009.

[31] H.Y. An, W.S. Choi, and S.G. Choi, "Real-time path planning for trajectory control in autonomous driving," In *2022 24th International Conference on Advanced Communication Technology*, pp. 154–159, 2022.

[32] P. Cai, Y. Lee, Y. Luo, and D. Hsu, "SUMMIT: A simulator for urban driving in massive mixed traffic," *2020 IEEE International Conference on Robotics and Automation*, pp. 4023–4029, 2020.

[33] S.R. Abhishek Nayak, K. Chour, T. Marr, D. Ravipati, S. Dey, A. Gautam, and S. Gopalswamy, "A distributed hybrid hardware-in-the-loop simulation framework for infrastructure enabled autonomy," *arXiv:1802.01787 [cs.RO]*, 2018, [Online]. Available: https://arxiv.org/abs/1802.01787

[34] D. Kapsalis, O. Sename, V. Milanes, and J. J. Martinez Molina, "Design and experimental validation of an LPV pure pursuit automatic steering controller," *IFAC-PapersOnLine*, vol. 54, no. 2, pp. 63–68, 2021.

[35] P. Polack, F. Altché, B. d'Andréa-Novel and A. de La Fortelle, "A real-time safe planning and control architecture for autonomous driving adapting to slippery roads," In *2018 21st International Conference on Intelligent Transportation Systems (ITSC)*, pp. 1688–1694, 2018.

[36] I.M. Zulhilmi, P.M. Heerwan, S.M. Asyraf, I.M. Sollehudin, and I.M. Ishak, "Experimental study on the effect of emergency braking without anti-lock braking system to vehicle dynamics behaviour," *International Journal of Automotive and Mechanical Engineering*, vol. 17, no. 2, pp. 7832–7841, 2020.

[37] Z. Abdullah, P.M. Heerwan, I.M. Izhar, and M.A. Zakaria, "Study the influence of distance in Artificial Potential Field (APF) for Autonomous Emergency Braking System (AEB) on longitudinal motion," In *IOP Conference Series: Materials Science and Engineering*, vol. 1068, no. 1, p. 012015, 2021.